CORE
Metadata, citation and similar papers at core.ac.uk
Provided by Institute of Transport Research:Publications

IAC-09-B1.2.2

IN-SITU EXPLORATION OF EARTH'S ATMOSPHERE USING NOVEL SPACECRAFT DESIGN

Farid Gamgami
Deutsches Zentrum für Luft-und Raumfahrt (DLR)
Institute of Space Systems, Robert-Hooke-Str. 7 28359 Bremen
Farid.Gamgami@dlr.de

Miriam Sinnhuber, Mathias Palm, Christian von Savigny,
Institut fuer Umweltphysik, NW 1 Otto Hahn Allee 1 28359 Bremen
miriam@iup.physik.uni-bremen.de, mathias@iup.physik.uni-bremen.de, csavigny@iup.physik.uni-bremen.de

Abstract

Altitudes between 40 and 140 km are not accessible for conventional aircraft and spacecraft for long-term duration. In particular the region around 100 km, the upper mesosphere and lower thermosphere (UMLT), is of great interest to scientists and engineers since it forms the transition from earth to space. Important physical phenomena take place at this region that have a strong influence on the atmospheric layers below. The scientific need to explore this region is very high. So far, the UMLT region has been accessible mainly to remote sensing observations, which are subject to vertical and horizontal smoothing of the measured information, and require an underlying model and possibly not existing a priori information about the subject of interest. Therefore, in-situ measurements in the UMLT region on a global scale would be of inestimable value. However any conventional spacecraft will quickly suffer from free molecular friction at UMLT altitudes, leading to rapid orbital decay. We intend to highlight the scientific need for in-situ measurements in the UMLT region and discuss several mission case studies. The impact of the special conditions at that altitude on the spacecraft design require a careful consideration.

1 Introduction

The atmosphere has been subject of intensive research in the past century. At the beginning this was done by ground-based methods, from balloons and airplanes. Later sounding rockets made higher altitudes accessible. These three means differ considerably from each other. Ground-based instruments provide only information about the column above the instrument but can provide very high time resolution. The measurements are usually subjected to vertical smoothing and may be affected by weather. Balloons have a restricted manoeuvrability and are limited to altitudes of less than ≈ 30 km. Airplanes are limited to much lower altitudes (≈ 12 km for conventional aircrafts, up to ≈ 25 km for high-altitude research and aerial reconnaissance aircrafts) but in contrast to balloons they are fully manoeuvrable. Sounding rockets on ballistic trajectories can reach ultimate altitudes of 800 km, but in contrast to their terrestrial counterparts, they provide only a small sampling time. These three systems all offer the capability to measure in-situ. In the last three decades, atmospheric

observations from satellite platforms have become more and more important. Satellite measurements have the advantage of obtaining a near-global picture of the atmosphere. However, below the cruising altitude of the satellite only remote sensing measurements are possible, which always average the measured signal along the line-of-sight or over a certain horizontal area, and are therefore subject to vertical and horizontal smoothing. Hence, no existing system is able to perform long-term global in-situ measurements at intermediate altitudes ($40 \leq h \leq 140$ km) so far.

This paper starts with a detailed discussion on the scientific need for in-situ measurements in the lower part of the thermosphere and the upper mesosphere, section 2. The scientific needs dictate the scientific requirements which themselves form the basis for the technical requirements. The special conditions and their impact on the vehicle at the altitudes of interest are dealt with in section 3. Two points deserve special consideration, the drag and the aerothermodynamic heating due to the rest-atmosphere. Hereafter several possible technical concepts will be introduced, section 4. The focus lies on the first concept, called AHAB. A feasibility and performance study will be given for the first and second concept.

2 Scientific Reasoning

Conventionally, altitudes below 100 km are referred to as "atmosphere" while everything above is "space". In fact, the altitude region of the upper mesosphere and lower thermosphere – roughly the altitudes between 70-120 km – form a borderline region which is affected both from the terrestrial surface and lower atmospheric layers as well as from extraterrestrial impacts.

Waves propagating up from the terrestrial surface and the lower atmosphere through the middle atmosphere break around the mesopause, transporting energy up from the surface into the upper mesosphere and possibly even into the thermosphere, thus delivering the power that drives the meridional circulation of the middle atmosphere. Anthropogenic or biogenic pollutants or greenhouse gases which are stable in the lower atmosphere are transported up into the mesosphere and lower thermosphere (MLT), where they are finally decomposed by oxidation or photolysis, changing the chemical composition of this region. This is certainly true for CO_2, which only decomposes into CO in the uppermost mesosphere and lower thermosphere [46].

The UMLT region is also affected by extraterrestrial impacts which can contribute greatly to the variability of chemical constituents, temperatures and dynamics there, but also affect the lower atmosphere due to large-scale downward transport during polar winter. In the MLT region, atmospheric constituents are decomposed and ionised by short-wave solar radiation in the far-UV to X-ray wavelength range. This is important e.g. for mesospheric water vapour photolysis by solar Ly-α radiation, which defines the amount of HO_x (H, OH) that ultimately controls the mesospheric ozone budget, but also as one source of ionisation in the lower thermosphere and uppermost mesosphere. As the short-wave solar radiation varies much more with solar activity than the visible and near-UV spectral range, the chemical composition of the MLT region will react more sensitively and quickly to solar activity than the lower atmosphere which is only reached by the near-UV, visible and IR fraction of the solar radiation. In the polar regions, precipitation of highly energetic particles – protons, electrons, α-particles from eruptions on the solar surface or from the terrestrial radiation belts – greatly affects the ion density during phases of enhanced geomagnetic activity. This is another source of ionisation of the UMLT region. As reactions of ions and neutrals are significantly faster than neutral-neutral reactions, ionisation also greatly disturbs the chemical composition of the upper atmosphere, leading to quite substantial and under certain conditions quite long-lived changes of the neutral composition. Especially

the formation of large amounts of HO_x and NO_x (N, NO) and subsequent ozone losses during large particle precipitation events in the mesosphere and stratosphere ([28],[29]) or due to geomagnetic activity in the lower thermosphere [4] should be mentioned here. Another source of extraterrestrial impacts into the atmosphere is the evaporation of meteorites, which takes place in an altitude range of $\approx$ 80-110 km. Evaporating meteorites supply the atmosphere with metal atoms which either ionise, forming metal ions, or oxidise, forming metal oxides. Metal oxides eventually recondense into tiny ($<$ 5 nm) particles, so called "meteoric smoke", which are presumed to act as nucleation nuclei for noctilucent cloud particles ([43] and [43]).

Changes in the chemical composition or dynamics of the UMLT region can affect the lower atmosphere; large long-lasting changes to the composition of the UMLT region will be transported downward into the lower atmosphere during polar winter, where they then affect chemical composition and possibly dynamics. This has been observed, e.g., for NO_x produced by energetic particle precipitation events during a number of polar winters in both hemispheres ([17], [42], [45]) and has also been modelled [32] and observed [13] for meteoric smoke. NO_x is – apart from halogen compounds – the most important species controlling ozone amounts in the mid-stratosphere; thus, NO_x from the UMLT region greatly influences ozone values in the polar mid-stratosphere [28]. Meteoric smoke particles have been implicated in a number of chemical processes in the stratosphere, as nucleation nuclei for stratospheric sulfate aerosols [38], in the production of HNO_3 in the upper stratospher during polar night [48], in the conversion of H_2SO_4 to SO_2 in the upper stratosphere [36], and even as nucleation nuclei for stratospheric clouds [32].

It has often been suggested that the upper mesosphere can act as an early warning system of climate change, which could be observed, e.g., in changes in the occurrence rate and brightness of noctilucent clouds (NLCs) at the cold polar summer mesopause ([14], [52]) . Long-term satellite observations of NLC albedo and occurrence frequency covering almost three solar cycles indeed show clear evidence of a positive trend ([49], [39]). However, observational evidence of mesospheric temperature trends is still highly ambiguous [19], [18].

A number of satellite-borne remote sensing missions has been launched in recent years which are at least partially dedicated and capable to perform measurements in the MLT region (e.g., AIM (Aeronomy of Ice in the Mesosphere [26], SABER on the American TIMED satellite [44], OSIRIS on the Swedish-Canadian-Finnish-French ODIN satellite, and to some extend the ENVISAT instruments GOMOS, SCIAMACHY and MIPAS ([6], [7], [24]). However, the UMLT region still remains the altitude region we know least about; considering the importance of the MLT region as a transition region between extraterrestrial impacts and the lower atmosphere, not much is known about this altitude region.

A very important property of the mesosphere and lower thermosphere is the propagation and breaking of gravity waves, and the resulting wave-structure of density and temperatures, which affect mesospheric and lower thermospheric dynamics and composition. This is currently investigated in a number of experiments, using ground-based LIDAR instruments (e.g. [34]) as well as space-borne passive remote sensing methods [2]. Two other MLT processes are of great interest, as they have the potential to impact also the lower atmosphere: (a) ionisation of the mesosphere and lower thermosphere, either due to photoionisation or precipitating energetic particles as the source of NO_x and ozone loss in the middle atmosphere; and (b) the evaporation of meteors, as the source of meteoric smoke particles. We propose to investigate the latter two points.

In order to investigate the ionisation of the MLT region several properties should be observed: the plasma density, which is a function of the atmospheric ionisation rate – this can be obtained, e.g., by measuring the electron density, as at altitudes

above ≈ 90 km no negative ions are formed, and electron density is essentially the ion density. Electron and ion densities, electron temperatures and potentials and can be measured using a Langmuir-sonde. Such probes have been flown on rocket experiments [10]. Another usefull parameter is the number density of nitrogen oxide, NO, which is produced by atmospheric ionisation. This can be observed by remote sensing using the γ-band emissions ([15],[47]). Other parameters of interest to specify the atmospheric background are the total air density, which again could be obtained from measuring the backscattered solar signal using a remote sensing instrument, and temperature, which may be measured indirectly using auroral emissions (e.g. via rotational temperatures of N_2 [31]). Both electron densities and nitrogen oxide are of interest throughout the upper mesosphere and lower thermosphere; electron densities above noctilucent clouds might also be of interest, as NLCs are often accompanied with regions of high radar echoes, the so-called polar mesospheric summer echos (PMSE).

To quantify the input of metals into the atmosphere, metals and metal ions in the altitude region around 100 km should be measured. This can be obtained by using mass spectrometry, providing measurements with a very fine horizontal resolution. Several aspects are of importance here. On the one hand, observation of the neutral metal species can provide information about the total influx of cosmic material into the atmosphere. Also, measuring the neutral and ionised compounds at the same time – possible either by using a sophisticated mass spectrometer, or by using additional information from a remote sensing instrument targeting the emission signals of the metals and metal ions – the partitioning between neutral and ionised compounds can be investigated. This will be particularly valuable if measurements of electron densities, neutral air density and temperature are also available. Another focus of interest is the occurrence of sporadic E-layers, layers of greatly enhanced metal densities which have been observed frequently from ground-based observations (e.g. [5], [21], [41]). Not much is known about their horizontal extent, as most observations have been from the ground, though recent spaceborne measurements suggest that they can extend over quite large areas [16].

Three types of instruments are proposed for this investigation: (A) a mass spectrometer to measure the metal and metal ion distribution with a very fine horizontal resolution; (B) a Langmuir-sonde for in-situ observations of electron and ion density fluctuations; and (C), a limb-viewing UV/visible grating spectrograph providing remote sensing observations of vertical metal, NO and OH concentration profiles, as well as neutral air density profiles and platform attitude information.

A satellite travelling in the UMLT region with high velocity will likely produce a substantial shock wave. This shockwave will change the density and temperature as well as the chemical composition of the atmosphere around the satellite; due to the high energy deposited into the surrounding air, a large amount of radiation will likely be produced as well [33]. This will affect the measurements, both from in-situ as well as from remote sensing instruments onboard a UMLT satellite; therefore, the design of the satellite plattform will have to consider this fact, and aim to minimise the impact of the bow shock.

3 Flow Physics

Flow physics in a technical sense is determined both by the condition of the medium and by the vehicle's motion. The upper atmosphere is first of all characterized by low density and low pressure. The density at higher altitude ($100 - 150$km) depends on several quantities like solar flux and geomagnetic activity. Each of these quantities varies with time on different scales. The longest time scale known is closely related the 11 year solar cycle. In addition to this well known influence, diurnal, seasonal and semiannual variations do oc-

cur. Moreover, there is not only a time dependence but also a spatial dependence. It has to be noted that modeling these effects causes uncertainties in the density-profile. An often used model atmosphere in orbit prediction and mission analysis is the Jacchia model J71 [27]. This is an empirical model which has the solar flux – represented by $F_{10.7}$ – and the geomagnetic index K_p as input variables. The model delivers temperature, composition and density. However, only the density is of sound physical meaning. The temperature and the molecular weight are intermediate results and do not represent reality precisely. It is interesting to note that by deriving this model atmosphere parameters have been adjusted by studying density induced orbit-decay, [35], although the C_D value of the involved spacecraft itself is subject of uncertainty.

At higher altitudes the density can vary by an order of magnitude depending on the solar activity. This is shown in figure 1. Three different density profiles are displayed; for low solar activity ($F_{10.7} = 70$, $K_p = 0.1$), medium activity ($F_{10.7} = 140$, $K_p = 2.2$) and high activity ($F_{10.7} = 220$, $K_p = 5$). Unless otherwise noted a medium solar activity was assumed for the upcoming results, section 5- 7. More sophisticated atmospheric models do exist but as this is a preliminary feasibility study the current degree of detail is sufficient. Though, a sound knowledge (i.e. modeling) of the atmosphere is essential for orbit prediction [30].

The density is of the order of $10^{-8}\,kg/m^3$ in the domain of interest leading to a high mean free path length (λ) of the molecules for which kinetic gas theory [11] gives:

$$\lambda = \frac{1}{\sqrt{2}} \frac{1}{\pi \sigma^2 n} \tag{1}$$

Here n is the particle density and σ denotes the cross-section of the molecules involved in a collision. The Knudsen number

$$Kn = \frac{\lambda}{L_v} \tag{2}$$

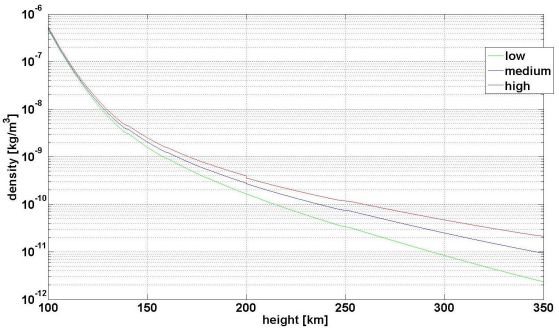

Figure 1: Density over height, after Jacchia atmosphere model

is defined as the ratio of the free molecular path length to a characteristic length of the considered vehicle. Expanding the fraction in equation 2 with the vehicle's velocity v leads to:

$$Kn = \frac{\lambda}{L_v} \cdot \frac{v}{v} = \frac{\lambda}{v} \frac{v}{L_v} = \frac{\Delta t_{\text{coll}}}{\Delta t_v} \tag{3}$$

This formulation reveals the physics stated by the Knudsen number: If the elapsed time between consecutive collisions of particles is much higher than the time an object (i.e. vehicle) needs to travel the distance L_v ($Kn \gg 1$), the particles do not have enough time to redistribute their momentum and the flow cannot be considered as a continuum. This state is called free molecular flow. Note that the Knudsen number is not a pure physical quantity because of the object's length scale in the denominator. The flow conditions around the 100 tons Space Shuttle at an altitude of 130 km for instance differ considerably from the flow around a compact 400 kg spacecraft. It is therefore important to mention the reference length scale for given Knudsen number. The different flow regimes depending on the Knudsen number are shown in table 1. Note that in most plots the free molecular flow

continuum	$0 < \text{Kn} < 10^{-2}$	$0 < \text{h} < 90\,\text{km}$
transitional	$10^{-2} < \text{Kn} < 10$	$90 < \text{h} < 140\,\text{km}$
free molecular	$10 < \text{Kn} < \infty$	$140 < \text{h} < \infty$

Table 1: Flow regimes depending on the Knudsen Number, $L_v = 2\text{m}$

regime is assigned to an altitude above 160 km [22] or even higher [11]. This is because of different macroscopic reference lengths, L_v. Figure 2 displays the mean free path in the altitude of interest. With a characteristic vehicle length scale of 2 meter, it follows that the Knudsen number is approximately 1.8 (120 km) and increases up to 20 (150 km). Hence the flow around a small spacecraft can already be considered as a free molecular flow from an altitude of 130 km upward. The range from 115 km to 130 km forms in the current study the transitional regime. This is important since both flow phenomena and computation methods are different for each regime.

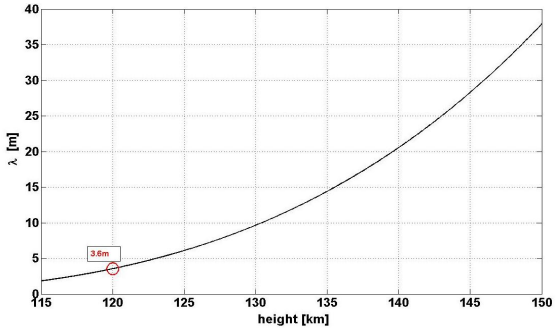

Figure 2: Free mean path λ plotted over height

3.1 Aerothermodynamics

The heat load, a classical problem for re-entry vehicles, is due to the very low density ($10^{-8} kg/m^3$) at 120 km altitude insignificant. However, it is less the suffering of the vehicle that matters but the suffering of the atmosphere. It is of utmost interest to know to what extent the vehicle's motion alters the unperturbed atmosphere. The fluid-vehicle interaction will alter the particle's degree of vibration, oscillation, excitation and even of ionisation depending on the involved species. The well known spacecraft-glow [12] is a striking evidence for such an interaction. This can be theoretically studied by direct simulation Monte-Carlo (DSMC). This method does not solve governing equations as it is the case in continuum flow mechanics. The interaction of particles with each other and with the vehicle's surface is directly modeled [1]. Albeit other methods that afford less computation power and demand less insight in the physical background exist, DSMC should be chosen to cover the transitional and free molecular flow regime.

It is of particular interest to investigate whether a bow shock will eventually form or not. Free molecular flow is per definition made up by particles that do not interact with each other. The formation of a bow shock as it is well known in continuum flow physics can not form in free molecular flows ($Kn \to \infty$). Hence the molecules are only affected by the encounter they experience with the spacecraft. Contrary to this, in a continuum flow regime, the fluid is dense enough to propagate by collision the information of an obstacle so that a shock front can form. However, the area of scientific interest (section 2) lies in between and demands special consideration.

Because of the preliminary character of the current study, no elaborate flow simulation has been performed yet but shall follow soon.

3.2 Drag Estimation

Usually the drag is modeled in a phenomenological way:

$$D = \frac{1}{2}\rho v_{\text{rel}}^2 C_D S_{\text{ref}} \tag{4}$$

with density ρ, relative velocity v_{rel} and reference surface S_{ref}. This Ansatz has proven to describe perfectly reality in continuum flow mechanics. But the application to rarefied flows is not straightforward [50]. The velocity in equation 4 has two contributions;

$$\vec{v}_{\text{rel}} = \vec{v}_{\text{sc}} + \vec{v}_{\text{atm}}. \tag{5}$$

The space crafts orbiting velocity and the velocity of the atmosphere. It is commonly assumed that the lower atmosphere rotates with the same angular velocity as the earth. However in higher altitudes winds of several hundred meter per

second can occur [20]. However very little is so far known about the mechanism of these winds. From equation 5 it is clear that a counter rotating space craft will experience (depending on the inclination) a higher relative velocity and hence a higher drag force.
In the following we will assume full validity of equation 4. In this case the decisive parameter is the drag coefficient C_D. A constant value of 2.2 is commonly in use. Though, Sentman [25] and Cook [9] showed in the sixties that the assumptions of a constant C_D is not valid and that the drag coefficient increases with height.
A proper calculation of C_D necessitates elaborated gas-surface interaction models (GSIM) which are in general incorporated in a direct simulation (DSMC). Hence, surface roughness and shape are important for the computation of C_D. Notice that such an elaborated simulation still requires pre-information to model various physical effects (e.g. accommodation parameter).
Rarefied flows demand indeed more effort to deal with than continuum flow mechanics, especially since a plethora of literature and codes exist for the latter one. The drag determination suffers from several sources of uncertainties; the density profile is only known to 10-15% and the drag coefficient depends on many factors which can not be modeled precisely. On account of this a sophisticated simulation was not attempted in this preliminary phase. Values based on a thorough literature study have rather been used since a feasibility study is aimed.

4 Technical Concepts

A system that allows long-term in-situ analysis in the flight critical domain (40-140 km) does not exist. Every system that stays permanently at this altitude range will suffer from violent orbital/altitude decay through drag of the rarefied atmosphere. To enlarge the flight life time every technical concept will require a propulsion system to overcome the drag or start with a large reservoir of total energy – or both. In principle three concepts are imaginable. The first concept that is in the focus of the current paper is a classical satellite (called AHAB) that is able to penetrate deeply into the atmosphere. A sound feasibility and performance study will be given for this conceptual design in section 5. The other two concepts are more unconventional. A wave rider type vehicle will be discussed in section 6 and first performance results can be given. The last concept considers two satellites that are connected with a tether. However, this is merely a suggestion since reliable results can not yet be presented for the latter.

5 A classical concept, AHAB

AHAB is an acronym, Atmospheric High Altitude proBe. Its base line is a classical earth observation satellite. AHAB shall have an eccentric orbit with a perigee of 120 km and an apogee of 800 km in order to enable in-situ measurements at low height. The impact of the rest-atmosphere on the satellite as discussed in section 3.2 is in many respects (satellite & mission) crucial.

Previous work Similar projects are; DAS and GEC. DAS [37] is a Japanese proposal from the late 70s and stands for Dive and Ascent Satellite. From a secure circular orbit (>300 km) the satellite shall occasionally dive into the lower layers of the atmosphere (115 km). GES stands for Geospace Electrodynamic Connection [23]. Depending on the scientific mission it consists of 2 to 3 satellites, that perform so called dipping campaigns (130-140 km) at the northern auroral regions. Similarly to DAS the dipping campaigns are deliberately initiated at specific moments. In this way the orbital lifetime can be drastically extended since the satellite returns to the safe almost drag-free initial orbit after such campaigns.

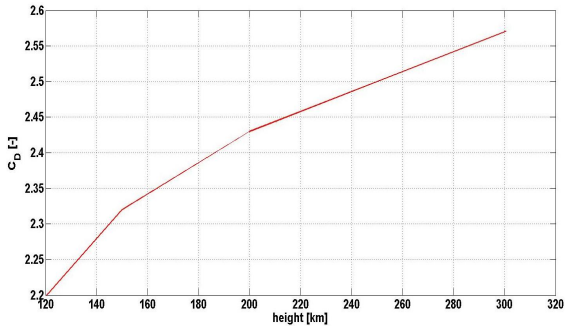

Figure 3: Height dependence of C_D

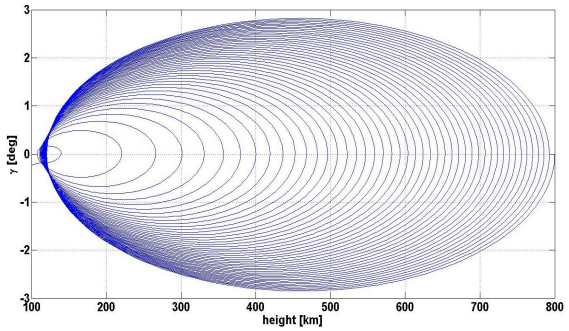

Figure 4: Phase-diagram for the un-propelled case

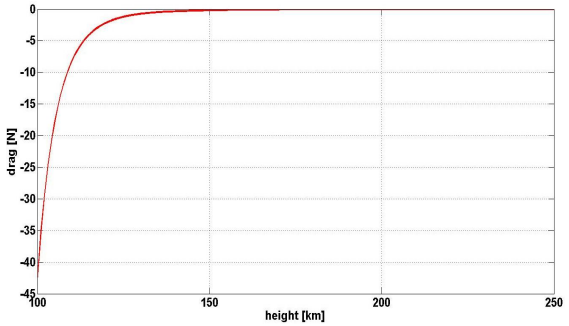

Figure 5: Drag over height for given base-line, table 2.

Performance analysis The base line of AHAB is displayed in table 2. Albeit no shape definition has taken place yet, we postulate a symmetric and compact satellite of elongated type. All acting forces generate torques if the line of action does go through the center of mass which changes the attitude of the vehicle. However, since the spacecraft's geometry is considered as symmetric and no angle of attack or side slip angle is foreseen, transverse forces and hence their torques are identically zero per definition. In principle there is the option of utilizing transverse forces for a deliberate orbit orientation change. This was not considered in this work. The satellites orbital plane lies within the equatorial plane and the simulation starts from the prime meridian. As discussed in section 3.2 we

mass	Orbit	C_D	S_{ref}
400 kg	120 x 800 km	f(height)	1m^2

Table 2: Base line of AHAB

do consider the height dependence of the drag coefficient. Following Sentman [25] we have a C_D over height as depicted in figure 3. In order to illustrate the atmospheric effects on orbit dynamics a pure ballistic probe shall be considered first. The extension of the orbital lifetime via a propulsion system and different thrust strategies will be discussed hereafter.

5.1 Ballistic Case

Figure 4 is a phase diagram depicting the flight path angle over height. The tendency of the drag to circularise an eccentric orbit by reducing the apogee is clearly visible. Notice that not only the apogee decreases but also the perigee. This is due to the finite impact of the drag force. Figure 5 shows the variation of drag with height. If the impact of the drag was not finite but a Dirac-function of an infinitely small impact-time, the perigee should not change – except periodically due to the zonal harmonics of the gravitational potential. The determining property for un-propelled trajectories is the ballistic coefficient:

$$BC = \frac{m_{\text{sc}}}{C_D(120\,\text{km}) \cdot S_{\text{ref}}} \tag{6}$$

With the spacecraft's mass m_{sc}, the drag coefficient C_D and the reference surface S_{ref}. The orbital life-

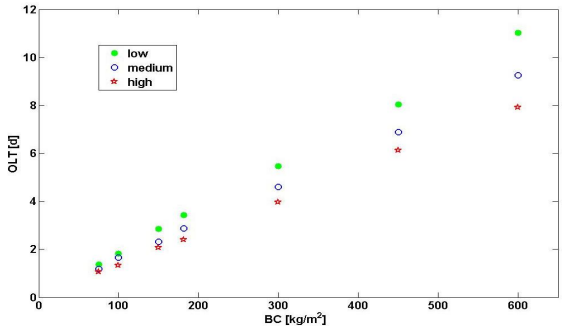

Figure 6: Orbital lifetime as a function of BC and solar activity as parameter

time increases with an increasing ballistic coefficient. This is shown in Figure 6. The rise in orbital lifetime with ballistic coefficient is almost perfectly linear. Moreover, the effect of density variation due to solar activity is also displayed in Figure 6. Naturally the orbital lifetime decreases with higher density. Interestingly the ratio:

$$OLT_{\rho,\text{high}} : OLT_{\rho,\text{medium}} : OLT_{\rho,\text{low}} = \text{const.}$$

is almost independent of the ballistic coefficient. The reason for this is the nearly linear relation of orbital lifetime to ballistic coefficient. Accordingly the orbital lifetime is decreased by 20% comparing the low density case to the medium density and medium to high density, respectively. In the following if not otherwise mentioned the atmosphere with medium solar activity will be used.

5.2 Thrust strategies

In order to increase orbital lifetime it is necessary to equip the spacecraft with a propulsion system. Several thrust strategies are possible: **(i)** The propulsion system is ignited to keep the predefined orbit of 120x800 km. Only small deviations will be tolerated. **(ii)** An orbit decay is deliberately tolerated. The spacecraft spirals down till the apogee reaches a certain height. Thrust is then given to re-establish the initial orbit, hence to increase the apogee. In both cases the propulsion system acts at perigee and apogee.

5.2.1 Thrust-Strategy I

The control of the orbit is given in that way:

- if $r_{ag} < r_{ag,\text{tol}} \Rightarrow$ ignite thrust at next perigee

and

- if $r_{pg} < r_{pg,\text{tol}} \Rightarrow$ ignite thrust at next apogee

In this way perigee and apogee are elevated if they fall below a specified border. The subscription *ag* stands for apogee, *pg* for perigee and *tol* for tolerable. The second control-law is very important since due to various effects (see section 5.1) the perigee decreases and the reason of orbital decay, the drag, increases exponentially. Table 3 subsumes the applied values: The spacecraft's configuration is not changed (see table 2). The task of the propulsion system is to overcome the drag of the rest-atmosphere and to elevate the perigee. A hydrazine motor is assumed with a specific impulse of 224s. Table 4 subsumes the mission-relevant propulsion parameters. Figure 7 displays the thrust strategy for the nominal space craft configuration and a certain section in time. It can clearly be seen that it is not necessary to activate the thrust every cycle. The satellites orbital lifetime can be extended from 2.8 days (ballistic case) to 18.3 days with 100 kg of propulsion which is one fourth of the overall mass. The dependence of orbital lifetime on propellant mass is shown in Figure 8. The increase in orbital lifetime with propellant mass is not exactly but almost linear.

$r_{ap,\text{initial}}$	$r_{ap,\text{tol}}$	$r_{pg,\text{initial}}$	$r_{pg,\text{tol}}$
800 km	790 km	120 km	118 km

Table 3: Nominal orbit and tolerable orbit

	thrust	pulse-time	momentum
perigee	15 N	100 s	1500 Ns
apogee	5 N	5 s	25 Ns

Table 4: Propulsion parameter

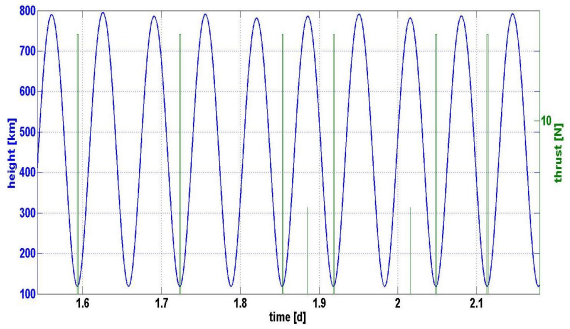

Figure 7: Height and thrust over time,thrust strategy I

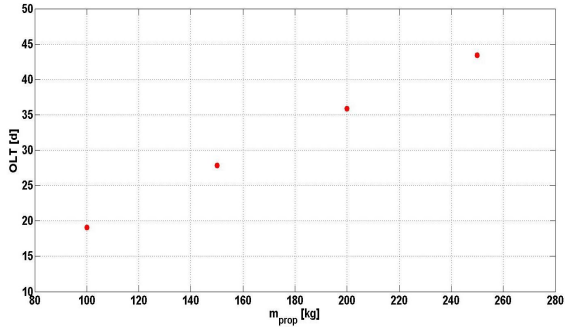

Figure 8: Orbital lifetime plotted versus propellant mass

5.2.2 Thrust-Strategy II

In the second mentioned thrust strategy the apogee drops down to 500 km and the orbit is elevated by means of a stronger propulsion system compared to thrust strategy I. A thrust of 400 N for a duration of 80 seconds is required. As in 5.2.1 a hydrazine motor with a specific impulse of 224s is assumed. Figure 9 illustrates this strategy by considering the transition section. Besides the large thrust momentum after 2 days many small thrust ignition phases are necessary to keep the perigee above 118 km.

5.2.3 Comparison

In table 5 both thrust strategies and the ballistic case are compared. The orbital lifetime can be increased by a factor of about 20 when a propulsion system is used. Moreover, it has been shown that thrust strategy I (i.e. keeping the spacecraft in close to the nominal orbit) is more efficient than thrust strategy II (spiraling orbit) by 10%. Both do have the disadvantage of polluting the environment which is subject of investigation with the propulsion exhaust. Hydrazin is a monopropellant that decomposes by a catalyst in a exothermic reaction into amonia, nitrogen and hydrogen.

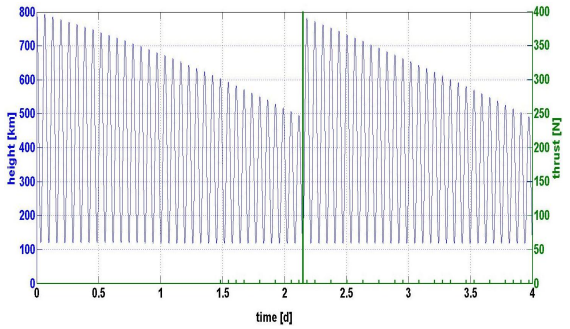

Figure 9: Height and thrust over time, thrust strategy II

	strategy I	strategy II	ballistic
OLT[d]	43.4	39.3	2.8

Table 5: Comparison of the discussed cases, $m_{prop} = 250\,kg$

$$3N_2H_4 \rightarrow 4NH_3 + N_2 \quad (7)$$

$$N_2H_4 \rightarrow 4N_2 + 2H_2 \quad (8)$$

A trade-off between both thrust strategies according the strength of pollution is necessary.

6 Skipping Concept (Orbital-Wave-Rider)

A wave rider type vehicle could be designed in a way to skip over the higher layers of the atmosphere. This can be considered as an extension of ordinary sounding rocket probes towards longer sampling times. Figure 10 shows such a trajectory. This was obtained by solving the equation of motion of a body with three degrees of freedom (3DoF). Main parameters and initial conditions are listed in table 6. The wave-rider type

mass	S_{ref}	h_{in}	γ_{in}	v_{in}
400 kg	$1.5m^2$	115 km	0.0717°	6.55 km/s

Table 6: Orbital wave rider initial condition

aircraft performs several skipping manoeuvres depending on the initial velocity and flightpath angle respectively. The initial velocity of 6.55 km/s is

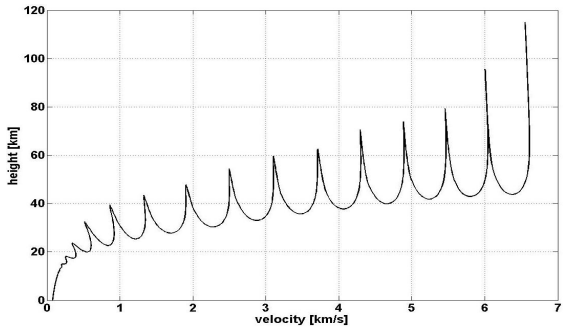

Figure 10: Entry trajectory of the orbital wave rider

very high and close to orbital speed. This value can be reduced but this has major impact on the trajectory. Figure 11 demonstrates this for the same configuration as in table 6 but with three different initial velocities. To hold all parameters constant and to vary only one is not ideal, though, sufficient to demonstrate trends of this modification. The pen-

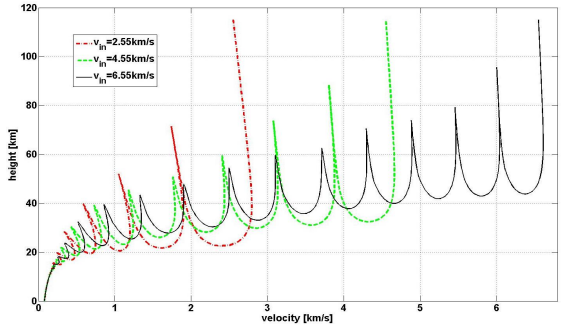

Figure 11: Entry trajectory for three different initial velocities

etration depth into the atmosphere increases with decreasing initial velocity. The number of skippings and the ratio of consecutive ultimate skipping heights decreases as well. The mechanical load increases up to a g-load factor of 10 for an initial velocity of 2.55 km/s. The penetration depth into the atmosphere increases with decreasing initial velocity. The number of skippings and the ratio of consecutive skippings decreases as well.

As for any lifting re-entry the lift over drag ratio is an important parameter. In the current case it directly determines the strength and hence the number of skipping manoeuvres. Naturally this factor cannot be chosen arbitrarily but is the result of a shape optimization process. In this preliminary state of investigation we followed the studies of the SpaceLiner[1] concept, see [51]. The aerodynamics of this hypersonic aircraft was investigated using surface inclination methods and the trimability of the whole vehicle was considered. Figure 12 shows the resulting lift to drag ratio over Mach number. The results are lower than expected

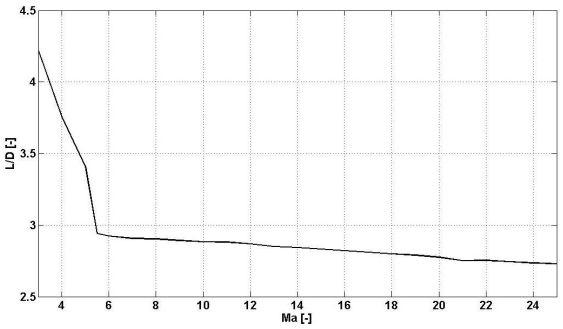

Figure 12: Actual L to D ratio over flight Mach number

if Kuchemann's [3] empirical relation for $(L/D)_{\max}$ in hypersonic flows is used:

$$(L/D)_{\max} = \frac{4(M_\infty + 3)}{M_\infty} \tag{9}$$

M_∞ denotes the free stream Mach Number. Note that other relations give a limiting value of 6 instead of 4. The reason for the discrepancy between equation 9 and figure 12 is easily explained considering the fact that Kuchemann's relation was

[1]This is a hypersonic aircraft that is able of carrying 50 passengers from Sydney to Western Europe.

derived for an aerodynamically optimally shaped wave rider, whereas the shape of the orbital wave rider deviates from the perfect wave-rider design because of the accommodation of scientific instruments and other technical subsystems. However, despite the possibility equation 9 might represent the L/D-barrier for hypersonic vehicle, the shape of the orbital wave rider has yet not been optimised. Hence the flight time can still be increased leading to a longer sampling time. The mechanical load on the vehicle is shown in 13. The maximum g-load factor does not exceed 3. With an elaborated guidance the skipping hight and the occurring loads can be improved considerably. However, this is beyond the scope of this preliminary study that that primarily aims at highlighting technical possibilities.

In this context two points deserve special consideration: **(i)** The design of a shape in order to investigate the trimability of this wave-rider-type probe is necessary. **(ii)** With a shape definition the thermal loads can be addressed properly.

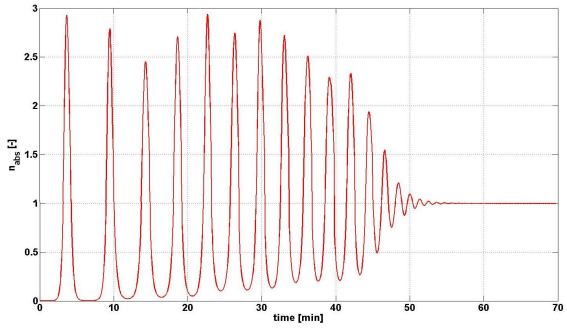

Figure 13: G-load factor over time

7 Tether aided Probe

This concept involves two satellites; a primary, the mother satellite, and a secondary satellite, the probe. Both shall be connected by a tether. The principle mechanism was first suggested by G. Colombo in 1974, [8]. The mother ship shall stay at an altitude of 150 km while the probe is deployed with a tether to an altitude of 130 km. The task of the mother ship is to boost the orbit, to control the attitude and to balance the torques that inevitably will occur. A detailed discussion on tethered satellite systems can be found in [40]. However this system faces many challenges, from control theory of a connected multi-body system to the mechanical and electrical charge of the tether. One very practical problem is the accommodation of a 20 km tether.

8 Discussion

Subject of this paper was twofold: First we tried to highlight the need of in-situ measurements in all heights of the atmosphere. Second, we pointed out that there is in aeronautical terms a gap in the atmosphere (40-140 km) that does not allow for a sustainable flight comparable to the regions below or above. We presented three concepts to make this *gap* accessible. First results for two concepts (AHAB and orbital wave rider) have been already presented. The third one (tether aided probe) was merely mentioned. The first one (AHAB) is based on a classical satellite orbiting the earth with a low perigee (120 km) and a high apogee (800 km). With a propulsion module the orbital lifetime can be extended to up to 40 days, depending on fuel amount and thrust strategy. The orbital wave rider is a hypersonic vehicle that skips over the higher layers of the atmosphere and extends the sampling time compared to a pure sounding rocket probe. For both suggestions only a basic feasibility study was aimed but the degree of detail and the area of disciplines shall be extended in further studies.

AHAB The aerodynamics and the question of the formation of a bow shock around a satellite deeply penetrating into the atmosphere is a vital question since the rest atmosphere will not stay unaffected. Only a sophisticated direct simulation (DSMC) can bring insight into this issue. From the system side a thorough mass estimation and a pre-

dimensioning of the related subsystems (i.e. energy supply) has to be performed to ensure a consistent design.

Orbital wave rider An analysis of the thermal load especially on a small vehicle is of great interest. A lower mass border given by the thermal protection system and the cooling mechanism determines the vehicles design. The perturbation of the atmosphere will be stronger than in case of AHAB. A bow shock will form definitely. If it is still possible to perform reasonable measurements is an open question.

References

[1] Bird G. A. *Molecular Gas Dynamics and the Direct Simulation of Gas Flows*. Oxford University Press USA, 2 edition, 1994.

[2] Chandran A., Rusch D. W., Palo S. E., Thomas G. E., and Taylor M. J. Gravity wave observations in the summertime polar mesosphere from the cloud imaging and particle size (cips) experiment on the aim spacecraft. *J. Atmos. Sol.-Terr. Phys.*, 71:392 – 400, 2009.

[3] John D. Anderson. *Hypersonic and High-Temperature Gas Dynamic*. AIAA, Reston, Virginia, 2 edition, 2006.

[4] D.N. Baker, C.A. Barth, K.E. Mankoff, S.G. Kanekal, S.M. Bailey, G.M. Manson, and J.E. Mazur. Relationship between precipitating auroral zone electrons and lower thermospheric nitric oxide densities: 1998-2000. *J. Geophys. Res.*, 106:24465–24480, 2001.

[5] T.J. Beatty, R.L. Collins, C.S. Gardner, C.A. Hostetler, C.F. Sechrist, and C.A. Tepley. Simultaneous radar and lidar observations of sporadic-e and na layers at arecibo. *Geophys. Res. Lett.*, 16:019–1022, 1989.

[6] J.L. Bertaux, E. Kyrölä, and T. Wehr. Stellar occultation technique for atmospheric ozone monitoring: Gomos on envisat. *ESA Earth Observation Quarterly*, 67, 2000.

[7] H. Bovensmann, J.P. Burrows, M. Buchwitz, J. Frerick, S. Noel, V.V. Rozanov, K.V. Chance, , and A.P.H. Goede. Sciamachy-mission objectives and measurement modes. *J. Atmos. Sci.*, 56:127–150, 1999.

[8] Grossi M. D. Colombo G., Gaposchkin E. M. and Weiffenbach G. C. Shuttle-borne skyhook, a new tool for low-orbital –altitude research. *Smithsonian Astrophysical Observatory, Cambridge, Massachusetts*, 1974.

[9] G. E. Cook. Satellite drag coefficients. *Planetary and Space Science*, 13(10):929 – 946, 1965.

[10] C. L. Croskey, J. D. Mitchell, M. Friedrich, F. J. Schmidlin, and R. A. Goldberg. In-situ electron and ion measurements and observed gravity wave effects in the polar mesosphere during the MaCWAVE program. *Ann. Geophys.*, 24:1267–1278, 2006.

[11] Hänel D. *Molekulare Gasdynamik*. Springer-Verlag, Berlin, 2004.

[12] Yee J-H. Dalgarno O. and LeCompte M. The atmosphere exploration and the shuttle glow. *Harvrad-Smithsonian Center for Astrophysics*, 1985.

[13] Hervig M. E., L. L. Gordley, L. E. Deaver, D. E. Siskind, M. H. Stevens, J. M. Russell III, S. M. Bailey, L. Megner, and C. G. Bardeen. First satellite observations of meteoric smoke in the middle atmosphere. *Geophys. Res. Lett.*, 2009.

[14] Thomas G. E., J. J. Olivero, E. J. Jensen, W. Schröder, and O. B. Toon. Relation between increasing methane and the presence of ice clouds at the mesopause. *Nature*, 338:490 – 492, 1989.

[15] F.G. Eparvier and C.A. Barth. Self-absorption theory applied to rocket measurements of the nitric oxide (0,1) gamma-band in the daytime thermosphere. *J. Geophys. Res.*, 97:13723–13731, 1992.

[16] Z. Y. Fan, J. M. C. Plane, and J. Gumbel. On the global distribution of sporadic sodium layers. *Geophys. Res. Lett.*, 34:15808–+, August 2007.

[17] B. Funke, M. Lopez-Puertas, S. Gil-Lopez, T. von Clarmann, G.P. Stiller, H. Fischer, , and S. Kellmann. Downward transport of upper atmospheric nox into the polar stratosphere and lower mesosphere during the antarctic 2003 and arctic 2002/2003 winters. *J. Geophys. Res.*, 2005.

[18] Beig G. Trends in the mesopause region temperature and our present understanding - an update. *Phys. Chem. Earth*, 2006.

[19] Beig G., Keckhut P., Lowe R. P., Roble R. G., Mlynczak M. G., J. Scheer, Fomichev V. I., Offermann D., French W .J. R., Shepherd M. G., Semenov A. I., Remsberg E. E., She C. Y., Lübken F.-J., Bremer J., Clemesha B. R., Stegman J., Sigernes F., and Fadnavis S. Review of mesospheric temperature trends. *Rev. Geo.-Phys.*, 2003.

[20] Coster A. J. Gaposchkin E. M. Evaluation of new parameters for use in atmospheric models. *Proceedings of 1987 AAS/AIAA Astrodynamics Conference. San Diego, CA: AAS-87-555 Publications Office.*, 1987.

[21] C.S. Gardner, D.G. Voelz, C.F. Sechrist, and A.C. Segal. Lidar studies of the nighttime sodium layer over urbana, illinois .1. seasonal and nocturnal variations. *J. Geophys. Res.*, 91:3659–3673, 1986.

[22] Benjamin P Graziano. *Computational modelling of aerodynamic disturbances on spacecraft within a concurrent engineering framework*. Dissertation, Cranfield University, 2007.

[23] J. M. Grebowsky and J. C. Gervin. Geospace electrodynamic connections. *Physics and Chemistry of the Earth, Part C: Solar, Terrestrial & Planetary Science*, 26(4):253 – 258, 2001.

[24] Fischer H. Mipas: an instrument for atmospheric and climate research. *Atmos. Chem. Phys.*, 8:2151–2188, 2008.

[25] Sentman L. H. Comparison of the exact and approximate methods for predicting free-molecular aerodynamic coefficients. *American Rocket Society*, 31:1576–1579, 1961.

[26] Russell III, James M., Scott M. Bailey, Mihaly Horanyi, Larry L. Gordley, David W. Rusch, Mark E. Hervig, Gary E. Thomas, Cora E. Randall, David E. Siskind, Michael H. Stevens, Michael E. Summers, Michael I. Taylor, Christoph R. Englert, Patrick J. Espy, William E. McClintock, and Aimee W. Merkel. Aeronomy of ice in the mesosphere. *J. Atmos. Solar-Terr. Phys.*, 2009.

[27] L. G. Jacchia. Revised static models for the thermosphere and exosphere with empirical temperature profiles. *SAO Special Report No. 332. Cambridge, MA: Smithsonian Institution Astrophysical Observatory.*, 1971.

[28] C.H. Jackman, E.L. Fleming, and F.M. Vitt. Influence of extremely large solar proton events in a changing stratosphere. *J. Geophys. Res.*, 2000.

[29] C.H. Jackman, D.R. Marsh, F.M. Vitt, R.R. Garcia, E.L. Fleming, G.J. Labow, C.E. Randall, M. Lopez-Puertas, B. Funke, T. von Clarmann, and G.P. Stiller. Short-and medium-term atmospheric constituent effects of very large solar proton events. *Atmos. Chem. Phys.*, 8:765–785, 2008.

[30] H. Klinkrad, G. Koppenwallner, D. Johannsmeier, M. Ivanov, and A. Kashkovsky. Free-molecular and transitional aerodynamics of spacecraft. *Advances in Space Research*, 16(12):33 – 36, 1995. Orbit Determination and Analysis.

[31] Junichi Kurihara, Takumi Abe, Koh-Ichiro Oyama, Eoghan Griffin, Mike Kosch, Anasuya Aruliah, Kirsti Kauristie, Yasunobu Ogawa, Sayaka Komada, and Naomoto Iwagami. Observations of the lower thermospheric neutral temperature and density in the DELTA campaign. *EARTH PLANETS AND SPACE*, 58(9):1123–1130, 2006. Japan Earth and Planetary Science Joint Meeting, Makuhari, JAPAN, MAY 22-26, 2005.

[32] Megner L., D. E. Siskind, M. Rapp, and J. Gumbel. Global and temporal distribution of meteoric smoke: A two-dimensional simulation study. *J. Geophys. Res.*, 2008.

[33] D. A. Levin, G. V. Candler, R. J. Collins, P. W. Erdman, E. Zipf, P. Espy, and C. Howlett. Comparison of Theory with Experiment for the Bow Shock Ultraviolet Rocket Flight. *J. Thermophys. Heat Transfer*, 7(1), 1993.

[34] Rauthe M., Gerding M., , and Lübken F.-J. Seasonal changes in gravity wave activity measured by lidars at mid-latitudes. *Atmos. Chem. Phys.*, 8:6775 – 6787, 2008.

[35] Bowman B.R. Marcos F.A. and Sheehan R.E. Accuracy of earth's thermospheric neutral density models. *AIAA*, page 2006–6167, 2006.

[36] M. J. Mills, O. B. Toon, C. E. Randall, and D. R. Marsh. Microphysical studies of mesospheric sulfate aerosol as PMC nuclei in WACCM3. *AGU Fall Meeting Abstracts*, pages A274+, December 2007.

[37] H. Mori, editor. *An onboard navigator for the extremely low altitude satellite DAS utilizing accelerometers*, August 1981.

[38] D. M. Murphy, D. S. Thomson, and M. J. Mahoney. In Situ Measurements of Organics, Meteoritic Material, Mercury, and Other Elements in Aerosols at 5 to 19 Kilometers. *Science*, 282:1664–+, November 1998.

[39] Shettle E. P., M. T. DeLand, G. E. Thomas, and J. J. Olivero. Long term variations in the frequency of polar mesospheric clouds in the northern hemisphere from sbuv. *Geophys. Res. Lett.*, 36, 2009.

[40] Penzo P.A. and Ammann P.W. *Tethers in Space Handbook*. NASA, Washington, DC, 76VVC7800000, 1989.

[41] J. M. C. Plane, R. M. Cox, J. Qian, W. M. Pfenninger, G. C. Papen, C. S. Gardner, and P. J. Espy. Mesospheric Na layer at extreme high latitudes in summer. *J. Geophys. Res.*, 103:6381–6390, 1998.

[42] C.E. Randall, V. L. Harvey, C. S. Singleton, S. M. Bailey, P. F. Bernath, M. Codrescu, H. Nakajima, , and J. M. Russell. Energetic particle precipitation effects on the southern hemisphere stratosphere in 1992-2005. *J. Geophys. Research*, 112:8308ff, 2007.

[43] M. Rapp and G. E. Thomas. Modeling the microphysics of mesospheric ice particles: Assessment of current capabilities and basic sensitivities. *Journal of Atmospheric and Solar-Terrestrial Physics*, 68:715–744, April 2006.

[44] J. M. Russell, M. G. Mlynczak, L. L. Gordley, J. J. Tansock, and R. W. Esplin. Overview of the SABER experiment and preliminary calibration results. In A. M. Larar, editor, *Society of Photo-Optical Instrumentation Engineers (SPIE) Conference Series*, volume 3756 of *Presented at the Society of Photo-Optical Instrumentation Engineers (SPIE) Conference*, pages 277–288, October 1999.

[45] A. Seppälä, P.T. Verronnen, M.A. Clilverd, C.E. Randall, J. Tamminen, V. Sofieva V, L. Backman L, and E. Kyrölä. Arctic and antarctic polar winter nox and energetic particle precipitation in 2002-2006. *Geophys. Res. Lett.*, 34, 2007.

[46] S. Solomon, R.R. Garcia, J.J. Olivero, R.M. Bevilacqua, P.R. Schwartz, R.T. Clancy, , and D.O. Muhleman. Photochemistry and transport of carbon monoxide in the middle atmosphere. *J. Atm. Sci.*, 42:1072–1083, 1985.

[47] M.H. Stevens. Nitric oxide gamma-band fluorescent scattering and self-absorption in the mesosphere and lower thermosphere. *J. Geophys. Res.*, 100:14735–14742, 1995.

[48] G. P. Stiller, G. Mengistu Tsidu, T. von Clarmann, N. Glatthor, M. Höpfner, S. Kellmann, A. Linden, R. Ruhnke, H. Fischer, M. López-Puertas, B. Funke, and S. Gil-López. An enhanced HNO_3 second maximum in the Antarctic midwinter upper stratosphere 2003. *Journal of Geophysical Research (Atmospheres)*, 110:20303–+, October 2005.

[49] DeLand M. T., Shettle E. P., Thomas G. E., and Olivero J. J. Latitude-dependent long-term variations in polar mesospheric clouds from sbuv version 3 pmc data. *J. Geophys. Res.*, 2007.

[50] Finkelman D. Vallado D. A. A critical assessment of satellite drag and atmospheric density modeling. *Paper AIAA 2008-6442 presented at the AAS/AIAA Astrodynamics Specialist Conference. Honolulu, HI.*, 2008.

[51] A. van Foreest, M. Sippel, and J. Klevanski. Technical background and challenges of the spaceliner concept, 2007. 7th International Symposium on Launcher Technologies, Barcelona, Spain.

[52] von Zahn U. Are noctilucent clouds truly a miners canary of global change? *EOS, Transactions American Geophysical Union*, 2003.